CHAPTER 3
Ultrasonography

YANG Wei Tse, Constantine METREWELI

INTRODUCTION

Ultrasonography (US) has expanded rapidly over the last two decades on a worldwide basis. The aims of this chapter are to describe the explosive growth of this field, the extensive applications of ultrasonographical techniques, and commonly encountered artifacts.

PHYSICS

Ultrasound waves are mechanical pressure waves similar to audible sound waves, and must have a medium in which to propagate. The frequency (*f*) is the number of high- or low-pressure regions crossing each area of tissue each second. The acoustic velocity (*c*) of an ultrasound wave is the wave velocity of the pressure waves travelling through the propagation medium.

The Asian-Oceanian Textbook of Radiology, 2003.
Edited by Wilfred C.G. Peh & Yoshihiro Hiramatsu.

Acoustic velocity is essentially frequency independent with an average value of 1540 metres per second. Most soft tissues in the body have acoustic velocities within 3% of this average. The acoustic wavelength (λ) is the basic repetition distance in space for a single frequency wave, joining points of equal phase. Due to their definitions, the wavelength and frequency of acoustic waves are related to each other by the following standard equation (true for all propagating waves)

$$c = \lambda . f \qquad [1]$$

Attenuation refers to the loss of strength of the acoustic waves as they travel through a medium.

Attenuation = beamwidth + scatter + absorption.

As the ultrasound frequency increases, the tissue attenuation gets stronger. Ultrasonic attenuation coefficients show that fat has the lowest value. Liver, kidney, and muscle are intermediate in value.

Bone has the highest value of attenuation. Due to its high impedance and attenuation, very little ultrasound energy transmits through bone and is represented in the ultrasonic image.

All transducers follow very specific rules in focusing. The focal length is the distance from the transducer face to the narrowest portion of the beam pattern. The focal zone is the range of axial distances over which the beam is sufficiently narrow to produce good image spatial resolution. A serious disadvantage of focused single-crystal transducers is that lateral blurring is only minimised over the length of the fixed focal zone, which can never cover the entire image field-of-view. Modern imaging equipment incorporates a variation of this scheme called multi-zone transmit-receive focusing, which enables all depths to be in focus in the same image. For each transmission, only the echoes coming from the focal zone would be acquired in receive; the rest would be ignored. When the results of these multiple separate transmissions are combined, a single effective beam pattern with good focus at all depths is achieved. Improved spatial resolution is accomplished with multi-zone transmit-receive focusing at the expense of temporal resolution because multiple transmissions are required for each image line. High quality real-time scanners use an even more complicated focusing scheme called dynamic focus, which takes advantage of the fact that receive-focus time delays can be continuously varied so that as echoes are being received, they are in focus.

Image spatial resolution comprises axial resolution (parallel to the beam central ray) and lateral resolution (perpendicular to the beam central ray). Axial resolution is determined by the pulse length of the ultrasonic signal. Lateral resolution is governed by the beamwidth of the transducer at the depth of the point reflectors, and is a consequence of the transducer scanning motion. Lateral resolution difficulties occur because of uncertainties in the lateral position of point reflectors in the beam. The vertical dimension of the image is governed by axial position uncertainties, and is an indicator of the pulse length at this depth. The horizontal dimension is governed by lateral position uncertainties, and is an indicator of the beamwidth at this depth. If two adjacent point reflectors are closer together than the beamwidth at their depths, their respective images will overlap, and they will not be identified in the image. However, if they are separated by a distance larger than the beamwidth, they will be easily separated (resolved) in the image.

Doppler effect

The Doppler effect is a change in frequency of received echoes (from that of the transmission pulse) due to target motion relative to the front face of the transducer (toward or away). If both the source and the receiver are stationary (at rest), then the received frequency (termed the effective frequency f_{eff}) is equal to the transmitted frequency f_o. In the usual clinical scenario with a stationary source and a moving receiver, the received frequency is given by

$$f_{eff} = \frac{C \pm V_r}{C} f_o \qquad [2]$$

In a pulse-echo ultrasonic measurement with the source and receiver being the same, the reflector motion causes a frequency difference between the received and transmitted frequencies

$$\Delta . f = \frac{2 . v . f_o}{C} \cos\theta \qquad [3]$$

where $\Delta . f$ = Doppler shift frequency
f_o = Transmitted frequency
V_r = Moving receiver velocity
V = Reflector velocity
θ = Angle between beam axis and V
C = Acoustic velocity

In continuous-wave (CW) Doppler ultrasound, the transmitted bandwidth of frequencies is very narrow, so very small reflector velocities with correspondingly small Doppler shifted frequencies can be detected. Because the output is continuous and not pulsatile, two separate transducer crystals must be used for transmission and reception. The prime use for CW Doppler equipment is in peripheral vascular studies where echoes from the red blood cells give a measure of blood velocities in blood vessels. For the range of reflector velocities found in the body (up to several hundred centimetres per second), the Doppler shift frequencies are all within the audible range. The amplitude of the audible Doppler signal is related to the number of reflectors in the sample volume. The pitch (frequency) of the audible Doppler signal is related to the velocities of the reflectors in the sample volume.

In pulsed Doppler equipment, a single transducer is time-shared in transmission and reception. A finite duration transmission pulse (tone burst) is emitted by the transducer, which will generate a continuous stream of echoes backscattered to the transducer. The received echo signals are then time-gated so that only a selected short distance along the transducer beam axis (range gate) is “listened to” by the equipment. This time gate may be placed at any depth along the transducer beam axis. Along with beamwidth at its depth, it determines the sampling volume of any moving reflectors. A clinical application of Doppler ultrasound is in the peripheral vascular system. By measuring the Doppler shift frequencies from the red blood cells, the spatial distribution of blood velocities inside the vessel may be determined if the sampling volume is much smaller than the lumen of the vessel. In the case of laminar blood flow, the velocity is greatest at the centre of the lumen and decreases to zero at the lumen wall because of viscosity effects. In the case of an artery, the time variation of the blood flow (velocities) with the cardiac cycle may be determined. If a plaque or other constrictions of the vessel lumen exist, then the Doppler measurement detects an increased velocity at the constriction. The presence of plaque sometimes causes non-laminar turbulent flow, which can be easily detected from the instantaneous Doppler shift frequency spectrum. Severe turbulence sometimes causes reverse inflow, which is also easily detected.

Duplex scanners combine a real-time imaging mode with a pulsed Doppler range-gated mode. Although duplex scanners provide a great deal of velocity information concerning one small region (sample volume) in the grey scale image, there is no velocity information provided concerning the other image points. Thus, the operator cannot be certain that the most diagnostically-relevant Doppler information has been acquired. With colour-coded Doppler, all (or most of) the imaged vascularity is surveyed, and estimates are obtained of the blood velocity. A range gate may then be placed at the most relevant image positions, and detailed blood flow Doppler data obtained.

REAL-TIME ULTRASONOGRAPHY

Ultrasound is produced by causing a special crystal to oscillate at a predetermined frequency. Very short pulses of sound lasting about a millionth of a second are transmitted approximately 500 times each second. The crystal transmits the pulses of sound and receives the returning echoes, which are electronically amplified and recorded as signals on a television monitor. Photographic reproductions of the image can provide a permanent record.

The time taken for each echo to return to the transducer is proportional to the distance travelled. Knowledge of the depth of the interface responsible for the echoes allows an image to be reproduced. It is possible to measure the distance between interfaces if the velocity of sound in tissues is known.

In diagnostic ultrasound examinations, high frequency sound is directed into the body from a transducer placed in contact with the skin. The skin is smeared with a gel-like substance to enable good acoustic contact. As sound travels through the body, it is reflected by tissue interfaces to produce echoes that are picked up by the same transducer and converted into an electrical signal. During the scan, the ultrasound beam is electronically swept through the patient's body, and a section of the internal anatomy is instantaneously displayed. Unlike other imaging modalities, there are no fixed projections. The production of the images and their subsequent interpretation are therefore highly operator dependent.

Fluid is a good conductor of sound, and US is therefore a particularly good imaging modality for diagnosing cysts, examining fluid-filled structures such as the bladder and biliary system, and demonstrating the foetus in the amniotic sac. Since air, bone and other heavily-calcified materials absorb nearly all the ultrasound beam, US plays little part in the diagnosis of lung or bone disease. The information from abdominal examinations may be significantly impaired by gas in the bowel, which interferes with the transmission of sound. US can also be used to demonstrate solid structures that have a different acoustic impedance from adjacent normal structures, e.g. metastases. US images are capable of providing highly detailed information and very small lesions (down to 3 mm) can be demonstrated.

Doppler effect

Sound reflected from a mobile structure shows a variation in frequency that corresponds to the speed of movement of the structure. This shift in frequency, which can be converted to an audible signal, is the principle underlying the Doppler probe used in obstetrics to listen to the foetal heart. The difference in frequency between the sound transmitted and received is known as the Doppler frequency shift. The Doppler effect can be exploited to image blood flowing through the heart or blood vessels. The sound is reflected from the blood cells flowing in the vessels. If blood is flowing towards the transducer, the received signal is of higher frequency than the transmitted frequency, while the opposite pertains if blood is flowing away from the transducer. The direction of blood flow can be readily determined and flow towards the transducer is by convention coloured red, whereas blue indicates flow away from the transducer. Doppler information in colour is superimposed onto a standard US image (Fig. 3.1). Flow velocity waveform can also be displayed and recorded (Fig. 3.2). As the waveforms from specific arteries and veins have characteristic

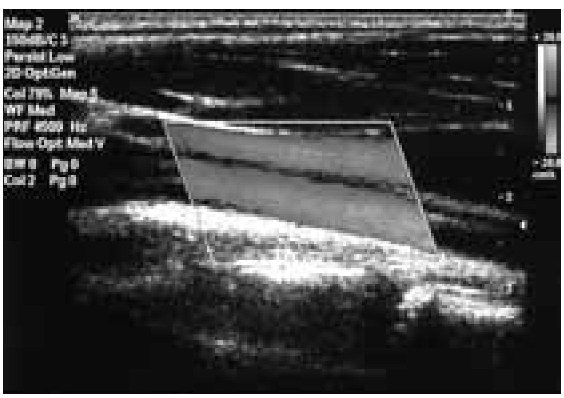

Fig. 3.1: Longitudinal colour Doppler scan of the neck shows the internal jugular vein, by convention coloured blue, indicating blood flowing away from the transducer, and the internal carotid artery, by convention coloured red, indicating blood flowing towards the transducer.

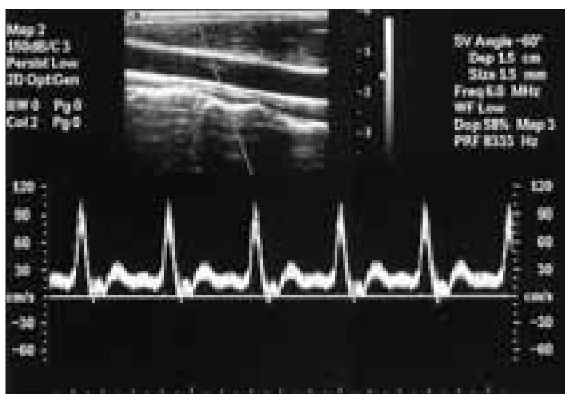

Fig. 3.2: Spectral Doppler trace of the carotid artery displaying the characteristic triphasic arterial waveform, obtained by placing the sample gate within the lumen of the vessel with angle correction of 60°.

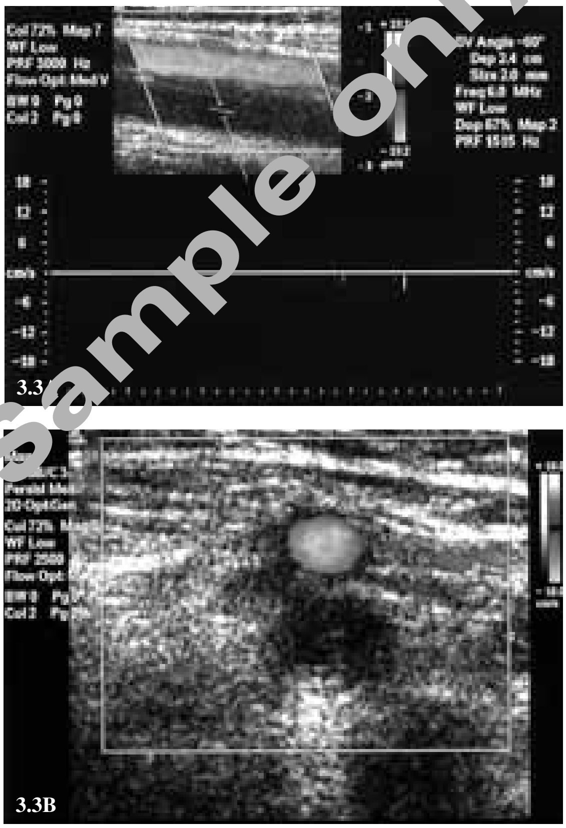

Fig. 3.3: (A) Longitudinal and (B) transverse colour Doppler duplex scans of the superficial femoral vein show an engorged vein with internal echoes and no colour flow suggesting deep vein thrombosis. The adjacent superficial femoral artery with normal flow is coloured red. Sample gate placed within the vessel lumen of the vein in fig. 3.3A shows absence of spectral waveform confirming thrombosis.

shapes, flow abnormalities can be detected. If the Doppler angle is known, then the velocity of the flowing blood can be calculated, provided the diameter of the vessel is also known [4].

Clinically, Doppler studies are used to detect venous thrombosis (Fig. 3.3), arterial stenosis and occlusion, particularly in the carotid arteries. In the abdomen, Doppler techniques can determine whether a structure is a blood vessel and can help in assessing tumour blood flow (Fig. 3.4).

A more recently-developed colour Doppler US technique is variously termed Doppler power imaging, power Doppler US, colour Doppler energy and colour power angiography (CPA) US, depending on the manufacturer. CPA US involves imaging the amplitude of blood flow rather than direction or velocity, as in conventional colour or pulsed Doppler US [5,6]. Imaging amplitude has several advantages. The most important is increased sensitivity to flow (Fig. 3.5) due to relative lack of angle dependence and the fact that noise has a low amplitude, which allows it to be filtered out, thereby allowing the operator to increase the gain. This feature also avoids the problem of aliasing.

Ultrasound contrast agents are currently available for clinical use [7,8]. These agents contain microscopic air bubbles that enhance the echoes received by the probe. The air bubbles are held in a stabilised form, so that they persist for the duration of the examination (See Chapter 2).

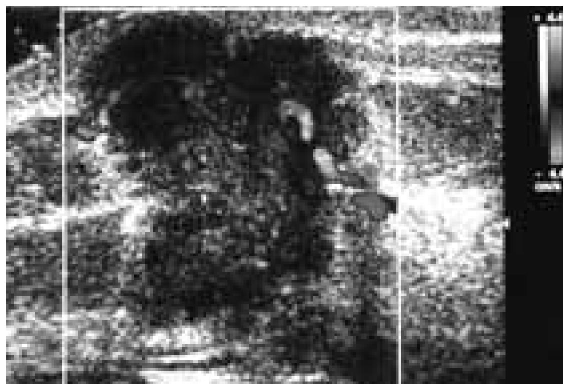

Fig. 3.4: Colour Doppler scan of a breast mass in antiradial plane shows florid intratumoral vascularity. Biopsy confirmed invasive ductal carcinoma.

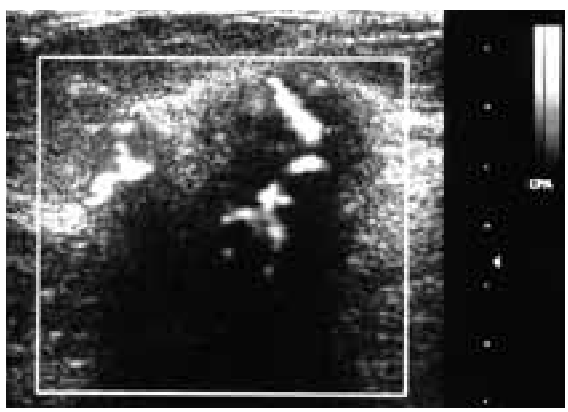

Fig. 3.5: Colour power angiography image of the same lesion as in fig. 3.4 shows intratumoral flow. Notice the increased conspicuity of tiny vessels within the lesion that is likely to be related to increased sensitivity of colour power angiography.

TRANDUCERS

Mechanical sector scanners

Mechanical sector scanners generally use single element transducers. The transducers are angled back and forth in an oscillatory motion such that the transducer beam defines a pie-shaped sector in the patient cross-section, with a limited field-of-view (FOV) for anterior structures and a widening FOV for more posterior structures.

Phased arrays

Phased arrays are sector scanners with no moving parts. A set of thin piezoelectric elements are arranged in a line, with their length along the slice thickness direction (perpendicular to the scan plane) and their thinnest dimension along the multi-element array axis.

Linear arrays

A linear array is also a linear arrangement of individual elements, but it is much longer and fires in a different manner from the sector array. Linear arrays form real-time images with a rectangular FOV.

Convex arrays

Convex arrays are a variant of the linear array design. They attain large sector-type FOVs at depth without side lobe difficulties and a loss of focus at the image edges.

Annular arrays

Annular arrays are an improvement on focused single crystal transducers. The transducer face is divided into a set of concentric ring elements. The rings can be electronically focused in much the same manner as the individual elements in a linear multi-element array.

Special probes

High-frequency transducers are useful in superficial small-parts imaging. The density of image lines in each frame, beamwidth, and pulse length governs image spatial resolution. With shallow FOVs, the transducer can be fired more often, resulting in more closely- spaced image lines. With this shorter penetration, higher frequency transducers may be used, resulting in tighter beam focusing (narrower beams) and better axial resolution for carotid, breast (Fig. 3.6), testis, and thyroid imaging (Fig. 3.7), hence yielding better images.

A recent advance is the development of very small probes that can be placed very close to the region of interest thus producing highly-detailed

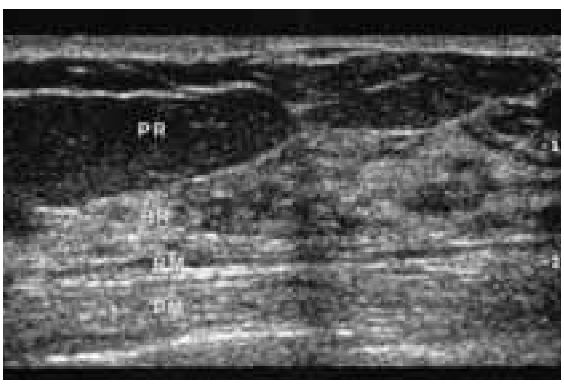

Fig. 3.6: Transverse grey scale image of the breast employing a high frequency (12 MHz) broad band transducer shows exquisite anatomical detail. (PR: premammary fat layer, BR: breast parenchyma showing stroma as white echogenic areas and ducts as dark linear areas, RM: retromammary fat layer, PM: pectoralis muscle).

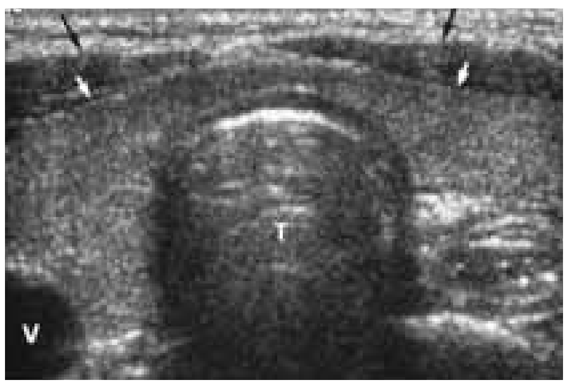

Fig. 3.7: Transverse grey scale image of the thyroid gland shows characteristic fine homogeneous echoes (white arrows). Anterior strap muscles are seen as thin sonolucent bands (black arrows). Air-filled trachea (T) in the midline gives a characteristic curvilinear reflecting surface with associated reverberation artifacts. (V: right internal jugular vein forms the lateral boundary of the thyroid gland).

Fig. 3.8: Transvaginal scan with a 7.5 MHz transducer shows a normal ovary (black arrows) with a dominant follicle (white arrow).

images but with a limited range of a few centimetres. Examples are rectal probes for examining the prostate and transvaginal probes (Fig. 3.8) for examining the pelvic structures [9,10]. Tiny ultrasound probes may be incorporated in the end of an endoscope. Lesions of the oesophagus, heart and aorta may be demonstrated with an endoscopic probe placed in the oesophagus, and lesions of the pancreas may be detected with an endoscopic probe passed into the stomach and duodenum [11,12]. Small intraoperative probes are frequently used in surgery [13]. Recently, both very small single-crystal transducers and multi-element arrays have been used to obtain very high frequency (20 MHz) scans of the arterial wall [14]. These intraluminal scans may prove to be effective in the detection and treatment of vascular disease.

ARTIFACTS

An artifact in imaging is used to describe unwanted information generated during the process of image formation [15,16]. They usually interfere with interpretation although there are occasional instances where they contain diagnostically useful clues (e.g. acoustic shadowing). Ultrasound is particularly prone to artifacts, therefore their recognition and avoidance form a major part of the skill and art of US [17].

Noise

Two types of noise beset all imaging systems, namely: random and structured. As electrical components produce random changes at low level, when these are amplified, they appear as a fluctuating, moving pattern of fine grey spots resembling a snow storm. Since the scanner's electronic components are designed to keep such noise at low levels, it is only seen when high degrees of amplification are applied. It is usually most obvious in the deeper parts of the image where the time-gain compensation (TGC) amplifier adds most to the overall receiver gain (Fig. 3.9). Because this type of noise is random in time, its effects can be reduced by

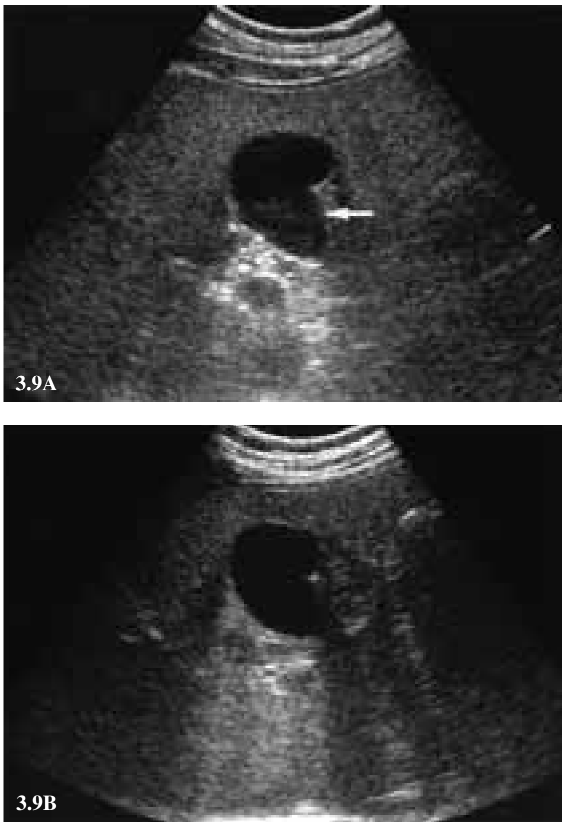

Fig. 3.9: Gain- related noise. (A) The combination of high overall gain and high time-gain compensation (TGC) amplification at depth may produce random noise in the image. This is present throughout the deeper parts of the image (white arrow). Because it is masked by the echoes from tissue structures, the noise is most obtrusive in echo-free regions such as within the gall bladder. (B) Correction of the excessive gains removes the noise.

temporal smoothing (the scanner controls for this are labelled frame averaging or persistence on some machines).

Random noise may also be produced by electrical interference, but in this case, it usually forms patterned signals such as flashes or bars in the image; structured noise such as this is known as clutter (Fig. 3.10). It is caused by pick-up of extraneous signals in the radiofrequency band by the transducer acting as an antenna, or by electrical pulses breaking through into the mains cable to interconnecting cables to attachments such as recorders. The noise they produce is usually easily recognised as being an artifact, the interference appearing randomly or intermittently, sometimes coinciding with the switching of a nearby motor or diathermy unit.

Scattering and specular interfaces

Two distinct types of ultrasound echo formation can be recognised, and each produces important artifacts. Echoes arising from small regions (around the ultrasound wavelength of 0.1 to 1 mm) where there is a change in impedance are known as scattered echoes because they are sent out more or less uniformly in all directions [18]. It follows that the amount of ultrasound energy returning to the transducer from each scattering structure is extremely low so that generally, this signal will be too weak to be detected. However, when an array of such weak scatterers lies in the beam (this is the usual situation when, for example, they are the surfaces related to liver lobules or renal tubules), their individual echoes combine to form an interference pattern, summing in some directions and subtracting in others. Signals strong enough to be detected are produced. The near-random pattern that results is known as speckle. The ultrasound pattern, though isotropic, is only remotely related to the real tissue structure: the displayed texture is actually a convolution of the real structure by the ultrasound beam

Fig. 3.10: Structured noise also known as clutter. Persistent oblique linear "raindrop" bars (white arrows) in this image were due to electrical interference to the scanner by nearby pneumatic drilling.

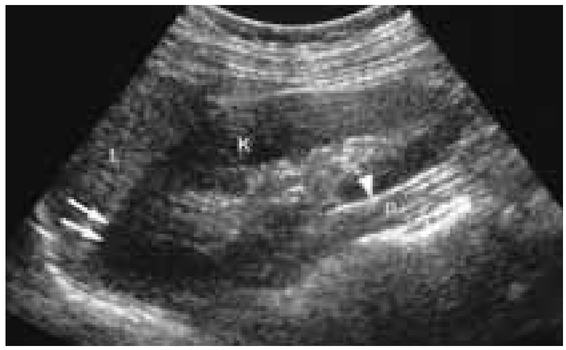

Fig. 3.11: Specular and scattered echoes. Scattered signals account for the generally low intensity parenchymal echoes from the liver (L) and kidney (K). Their appearance is independent of the direction of the ultrasound beam. Specular echoes arise from the flatter structures of the peritoneal and fascial layers separating the kidney from the psoas muscles (P). These echoes are strongly dependent on the angle between the beam and the surface, being intense when the surface is aligned at 90º (arrowhead) but weak or even completely absent when the beam runs along the interface (white arrows).

characteristics. Because the speckle pattern can be produced by the transducer as well as by the tissue, the same organ will produce a different texture with different transducers so that organs with different histological structures may have indistinguishable appearances on US, e.g. near-identical texture of the liver and spleen. When the reflecting surface is flat (relative to the ultrasound wavelength), it behaves as a mirror so that the direction of reflection equals the angle of incidence.

Since the focused beam of ultrasound is not dispersed, all reflected energy can be picked up by the transducer so that the signals are much stronger than for scatterers. However, they are intensely directional and can only be detected when the transducer is correctly situated, i.e. when the surface is at right angles to the beam for the standard pulse-echo imaging. As the surface is tilted away from the right angle, the signal intensity falls off rapidly (Fig. 3.11). In practice, most interfaces are detectable up to angles of more than 60º albeit with diminished intensity depending on the particular structures involved. However, beyond some limiting angles, that surfaces are not imaged and this can be most confusing. It accounts for the apparent communication sometimes seen between the inferior vena cava and the aorta when these lie close together, for the failure to image the sides of the globe of the eye, and for the invisibility of the superior surface of the urinary bladder in ascites scanned from certain angles. Such missing surfaces can always be scanned from other angles, i.e. the ultrasonographer needs to be aware of the problem to avoid serious diagnostic errors.

Fig. 3.12: Acoustic shadowing. When a structure absorbs more sound energy than its surroundings, the TGC correction is inadequate for the region and the deeper structures appear darker – this is known as acoustic or distal shadowing, here produced by gallstones in the gall bladder (white arrow).

Shadowing and enhancement

The commonest forms of shadowing (and its counterpart, enhancement) are perhaps not true artifacts and their presence provides important diagnostic information about the attenuation of the tissues responsible for them [19]. The types of shadowing include attenuation (attenuation higher than TGC compensation), reflective (near-total reflection) and edge (from curved surfaces). Shadowing from attenuation occurs when a region of the tissue has a higher attenuation coefficient than the majority of the tissues in the scan, since the TGC (which corrects for the attenuation with depth) can only be applied to this region so that both it and the tissues deep to it are depicted as less reflective than they actually are (Fig. 3.12). Since shadowing implies loss of acoustic signal for a tissue region, it can also be produced by an extremely efficient reflector such as a gas bubble, fatty tissue or region of calcification where much of the incident sound beam is reflected back, respectively (Fig. 3.13). It casts an acoustic

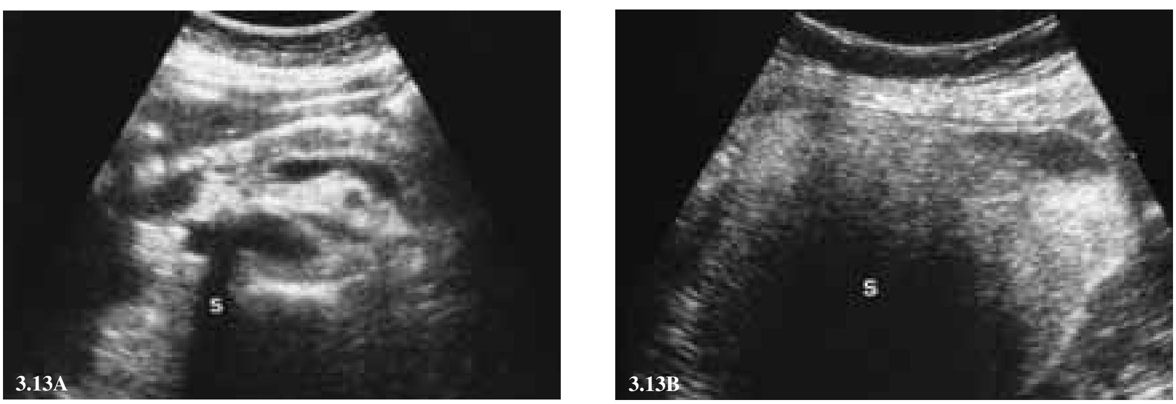

Fig. 3.13: Reflective shadowing. When an interface reflects all or almost all of the incident sound energy, a situation that is typical of (A) gas or (B) fat, so little penetrates that a band of distal shadowing (S) results. Though the effect is the same as with acoustic shadowing (compare with fig. 3.12), the mechanism is different.

shadow because very little of the energy penetrates to insonate the deeper tissues.

For most soft tissues, only a small proportion of the loss of energy from the beam (attenuation) is due to reflection so that echogenicity does not correlate well with attenuation. Interesting and confusing shadows are seen deep to the edges of strongly-curved surfaces such as vessels and cyst walls (Fig. 3.14). Edge shadows are fine echo-poor lines extending deep to the edges of strongly-curved structures. Two possible mechanisms are illustrated. The beam is dispersed as it reflects from the curved edge which is struck at more than the critical angle; the returning echoes from the spreading beam have less energy than echoes from a confined beam so that, even though they are reflected

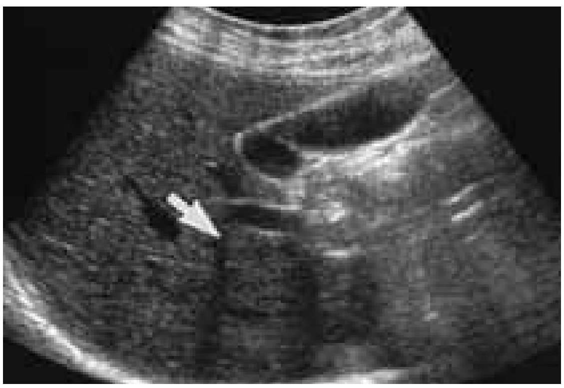

Fig. 3.14: Edge shadows. Edge or refractive shadows are commonly produced by smooth curved surfaces. Such a shadow is seen beyond a fold in the gall bladder (arrow). The curved surfaces of solid structures can also produce edge shadows.

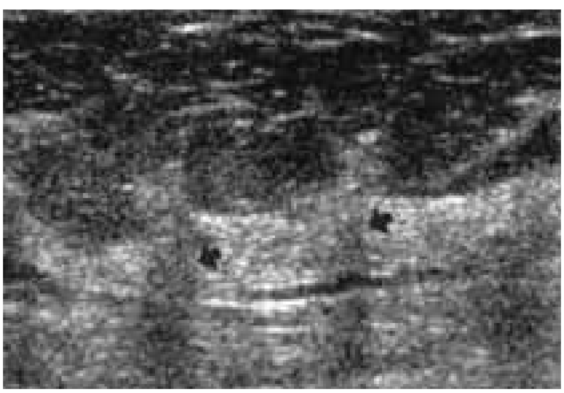

Fig. 3.15: Edge shadows are seen posterior to Cooper ligaments in the breast (black arrows).

Fig. 3.16: Enhancement. The fluid in a cyst absorbs very little of the sound energy passing through it so that the TGC, which has been adjusted to correct for attenuation in the surrounding tissue (the liver in this case), is locally excessive. The deeper tissues are depicted as being more reflective, giving a lighter band (arrows) known as distal or acoustic enhancement.

from the interfaces they encounter, their intensity is reduced. The importance is that edge or refractive shadows do not have the same diagnostic significance as bulk shadowing. They are commonly seen in situations where shadowing alerts to the presence of calcification (e.g. from the walls of the renal sinus) or of sinister lesions (e.g. from Cooper ligaments of the breast) (Fig. 3.15). They must therefore be recognised for what they are and dismissed.

Conversely, if a region of tissue attenuates less than its surroundings, echoes from it and deeper tissues are over-corrected and appear as a bright band known as "enhancement" (Fig. 3.16). This enhancement has no relation to the increase in tissue contrast produced by the injection of "contrast agents", e.g. iodinated compounds in conventional radiology. Echogenic fluids (e.g. crystalline bile or a pyonephrosis) are examples where strong echoes are associated with enhancement (Fig. 3.17).

Multiple echoes

The ultrasound beam generally returns directly to the transducer after a single reflection in pulse-echo ultrasound. Where the geometry allows multiple reflections to occur, multiple images are formed, sometimes to rather confusing effect. Repeat echoes are likely to occur where the reflections are strong and this implies flat surfaces giving specular echoes. Since the path lengths for multiples are longer, the corresponding images are depicted as lying deeper in the body, and they are weakened as the ultrasound is attenuated. Therefore, multiple echoes are more likely to be observed when the surfaces are close together and when the intervening tissue is of low attenuation, especially when it is fluid. An example of a single repeat echo is the mirror image artifact where a repeat image of a structure is depicted on the "other side" of a specular reflector and equidistant from it [20]. This effect is readily demonstrated for the diaphragm: imaged from below through the liver, echoes commonly appear above the diaphragm (Fig. 3.18), and occasionally discrete structures in the normal liver or focal lesions can be recognised. This is not the appearance of the lung and is attributable to the beam reflecting back into the liver from the diaphragm [21]. The reflecting surface is likely the air/pleura interface as the muscle of the diaphragm itself would be expected to act as a scatterer rather than a specular reflector. A situation where the mirror artifact is confusing is the repeat echo of the bladder in the pelvis which may mimic an echo-poor mass. The simulated deep interface forming the back wall of a pseudomass is

Fig. 3.17: Enhancement is also noted posterior to dilated bile ducts (white arrows) which contain crystalline bile.

derived from the typical geometry. Anatomical impossibility, and lack of cephalad and caudad margins with strong anterior and posterior margins, should alert the ultrasonographer to the diagnosis of this artifact.

Multiple repeat echoes are known as reverberations, and are produced when two strong reflectors lie parallel to each other. Common examples include gas bubbles or stones parallel to the skin surface where the skin/transducer interface forms the second reflector (Fig. 3.19A). A striped pattern results, with the deeper multiple echoes becoming weaker because of loss of sound energy due to incomplete reflection at the surfaces and to attenuation by the intervening tissues. Since weaker echoes

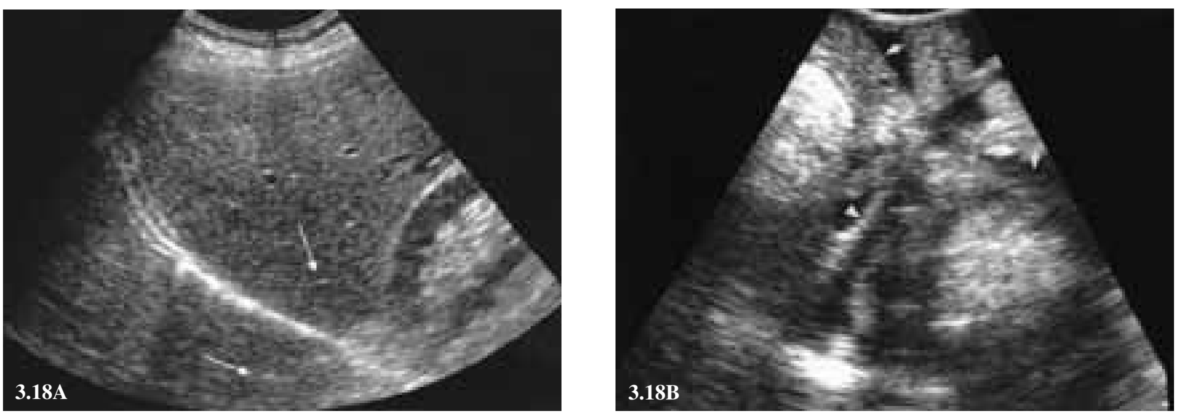

Fig. 3.18: (A) The "mirror image artifact" due to reflection of echoes across the diaphragm (arrows). (B) Another example illustrates reflection of echoes from an ovarian dermoid (white arrows) across the peritoneal membrane (arrowhead) during laparoscopic US.

appear to be narrower than stronger ones, the reverberating bands become shorter as well as less intense with depth (Fig. 3.19A). A bright streak appears on the display, forming a tail distal to the image of the causal structure which is itself usually strongly reflective. The whole complex looks rather like a comet with its tail (Fig. 3.19B). This is commonly seen with foreign bodies such as surgical clips, implants (including intra-uterine devices) and catheters, and small fluid cavities such as the Aschoff-Rokitansky sinuses in the wall of the gall bladder in adenomyosis.

Velocity errors

An important assumption of scanners is that the velocity of ultrasound in soft tissues is constant. Changes in velocity produce refractive artifacts; the ultrasound beam deviates from its straight line path when it crosses obliquely between two tissues of different velocity. The beam is bent towards the 90º line when entering a slower tissue. The degree of displacement depends both on the speed of sound difference and on the distance of the object from the surface. This lateral distortion is particularly important in pelvic scans by the abdominal route. The beam crossing the wedge-shaped fat space around the rectus muscle is refracted so that deep pelvic structures (e.g. the uterus or prostate) can appear stretched laterally [22, 23]. The "split image" artifact is less common in the upper abdomen, perhaps because there is usually less fat and less muscle, but occasionally apparent duplication of the coeliac axis is seen (Fig. 3.20). Refraction of the ultrasound beam by the fatty tissues in the anterior abdominal wall can produce split or double images such as an apparent double intra-uterine contraceptive device (IUCD) in the uterus. The distortional displacement disappears when the transducer is moved so as to image the pelvis through the centre of the muscle.

Fig. 3.19: (A) Reverberation artifacts due to reverberation by gas in the duodenum/pylorus (arrow). (B) Comet tail artifact (arrowhead) due to gas in the uterine cavity.

Beam width

The real ultrasound beam shape falls far short of the desired uniformly-thin laser beam configuration that would be optimal. A typical actual focused beam consists of a disturbed region immediately in front of the transducer surface, then a near zone that progressively narrows to the focus, after which it spreads in the far zone. In addition to this main beam, there are side lobes, low energy beams directed at angles away from the centre line. Axial resolution depends on the pulse length that is mainly determined by the wavelength which may be 0.3 mm for a 5 MHz transducer and does not change significantly with depth. In contrast, the width of the main beam defines the lateral resolution of the ultrasound image because adjacent objects can only be separately resolved if the beam is narrower than the distance between them [24].

Fig. 3.20: Refractive artifacts. Refraction of the ultrasound beam by the fatty tissues in the anterior abdominal wall can produce split or double images such as the apparent duplication of the gastroduodenal artery (arrows).

If the beam is wider, they are depicted as one larger object on the screen. Lateral resolution varies with depth, being best at the focal zone and deteriorating rapidly beyond it. The edges of the beam are not sharply-defined; the ultrasound energy is concentrated on the centre line of the beam, and falls off progressively from the centre line with a Gaussian distribution. This means that a strong reflector will continue to give detectable echoes further from the central axis than a weak reflector. In clinical terms, this means that the resolution of ultrasound is better for weak reflectors. Strong reflectors tend to blur laterally, and are therefore seen as cigar-shaped smears or streaks so that their width is exaggerated. This is the beam width artifact and is most obvious when the smearing overlaps an echo-free structure, often encountered when a gassy or bony structure lies adjacent to a fluid space (Fig. 3.21). Beam width artifacts also occur in the orthogonal plane, i.e. across the slice thickness. With circular transducers, the beam is symmetrical in all planes but for linear and phased arrays, the beam is wider in the orthogonal plane. Orthogonal beam spread artifact is exactly the same as the slice thickness artifact in CT except that the ultrasound beam is non-uniform. Low level information derived from signals in adjacent planes is spuriously depicted in the image plane [25]. Typically, echo-poor bands or lines are noted within echo-free spaces. They may mislead the operator into thinking the fluid contains debris.

INVASIVE PROCEDURES

The advantages of ultrasonographical guidance of abdominal aspiration or drainage procedures include real-time visualisation of the needle or drainage catheter as it passes into a target area which allows direct precise needle placement in critical areas, with avoidance of intervening structures

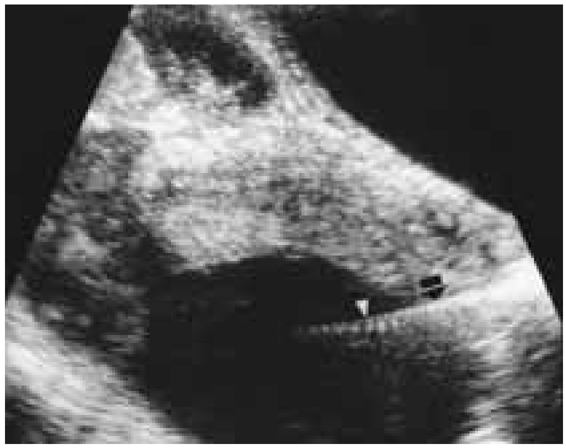

Fig. 3.21: Beam width artifact. Echoes arising from structures at the edge of the ultrasound beam, which has a finite width, are depicted as lying in the centre-line of the beam. In this example, the strong echoes from a pocket of gas in a pelvic gut loop (broken black arrow) smear across the bladder (white arrowhead).

Fig. 3.22: Ultrasound- guided fine needle aspiration of a breast mass. Notice the needle shaft (arrows) with its tip within the centre of the mass. Final pathology was a fibroadenoma.

(Fig. 3.22), as well as real-time confirmation of drainage. Ultrasound-guided aspiration is expedient and the time required for the procedure is relatively short. Portability of ultrasound units alleviates the risk and inconvenience of transporting a critically ill patient. The utility of pulsed Doppler US or colour flow imaging aids in preventing complications of aspiration or biopsy by identifying the vascular nature of a mass, and in avoiding vascular structures lying within the needle path. The major disadvantages include poor visualisation because of overlying bowel gas that may obscure the deeper structures, and limitation by bone, drains or dressings.

Needle biopsy and aspiration

Ultrasound- guided biopsy is utilised for the following purposes: determination of abscess versus tumour, determination of a fluid-filled mass versus a solid tumour, determination of malignancy of a mass [26], and verifying the presence and type of renal parenchymal disease. Visualisation of the biopsy needle requires that it traverses the ultrasonographical scanning plane. This may be accomplished by attaching a biopsy guide to the transducer or by the freehand technique. A sterile sheath must be placed over the transducer and any biopsy attachment used prior to starting the procedure. Larger needles are more easily seen with ultrasound than smaller needles, and teflon- coated needles are generally easier to visualise than noncoated needles. With small or poorly- visualised needles, it may be possible to determine the needle location by observing the motion of the needle in real-time as the physician advances it toward a target. US can also be used to monitor real- time the size of a fluid-filled mass during drainage. Ultrasound-guided aspirations are used for the following purposes: distinguish between a fluid-filled mass and a solid mass, determine if a fluid-filled mass is an abscess, determine if a fluid-filled mass is benign or malignant, confirm the diagnosis of haematoma, and also for pseudocyst, abscess, and biloma drainage.

Treatment

US- guided percutaneous ablation of liver tumours has recently been performed using a variety of therapeutic modalities, including alcohol injection, laser photocoagulation, radiofrequency ablation and microwave coagulation [8, 27-30].

REFERENCES

1. Chivers RC, Parry RJ. Ultrasonic velocity and attenuation in mammalian tissues. J Acoust Soc Am 1978; 63:940-953.
2. Goldstein A. Ultrasonic imaging. In: Webster JG, ed. Encyclopedia of Medical Devices and Instrumentation. New York: John Wiley & Sons Inc, 1988.
3. Goldstein A. Range ambiguities in real-time ultrasound. J Clin Ultrasound 1981; 9:83-90.
4. Taylor KJW, Holland S. Doppler ultrasound. I. Basic principles, instrumentation and pitfalls. Radiology 1990; 174:297-307.
5. Rubin JM, Bude RO, Carson PL, Bree RL, Adler RS. Power Doppler US: a potential useful alternative to mean frequency-based color Doppler US. Radiology 1994; 190:853-856.
6. Martinoli C, Derchi LE, Rizzatto G, Solbiati L. Power Doppler sonography: general principles, clinical applications, and future prospects. Eur Radiol 1998; 8:1224-1235.
7. Frauscher F, Janetschek G, Helweg G, et al. Crossing vessels at the ureteropelvic junction: detection with contrast-enhanced color Doppler imaging. Radiology 1999; 210: 727-731.
8. Solbiati L, Goldberg SN, Ierace T, et al. Radio-frequency ablation of hepatic metastasis: postprocedural assessment with a US microbubble contrast agent – early experience. Radiology 1999; 211:643-649.
9. Fleischer AC. TVS claims diagnostic role in ovarian cancer. Diagn Imaging 1988; 10:124-128.
10. Lee F, Littrup PJ, Kumasaka GH, et al. The use of transrectal ultrasound in the diagnosis, guided biopsy, staging and screening of prostate cancer. RadioGraphics 1987; 7:627-644.
11. Chak A, Canto M, Gerdes H, et al. Prognosis of esophageal cancers preoperatively staged to be locally invasive (T4) by endoscopic ultrasound (EUS): a multicentric retrospective cohort study. Gastrointest Endosc 1995; 42:501-506.
12. Rosch T, Braig C, Gain T, et al. Staging of pancreatic and ampullary carcinoma by endoscopic ultrasonography. Comparison with conventional sonography, computed tomography, and angiography. Gastroenterology 1992; 102:188-199.
13. Rifkin MD, Rosato FE, Mitchell Branch H, et al. Intraoperative ultrasound of the liver: an important adjunctive tool for decision making in the operating room. Ann

Surg 1987; 205:466-471.

14. Yucel, EK, Waltman AC. Ultrasound-tipped catheter views arteries from inside. Diagn Imaging 199[illegible]; [illegible]4:108-111.
15. Laing FC. Commonly encountered artifacts in clinical ultrasound. Semin Ultrasound 19[illegible]; [illegible]1-25.
16. Kremkau FW, Taylor KJW. Artifacts in ultrasound imaging. J Ultrasound Med 1986; [illegible]-237.
17. Sanders RC. Atlas of Ultrasonographic Artifacts and Variants. Chicago: Year Book, 1986.
18. Wells PNT, Halliwell M. Speckle in ultrasonographic imaging. Ultrasonics 1981; 19:225-232.
19. Suramo I, Paivansalo M, Vuoria P. Shadowing and reverberation artifacts in abdominal ultrasonography. Eur J Radiol 1985; [illegible]147-151.
20. Cosgrove DO, Garbutt P, Hill CR. Echoes across the diaphragm. Ultrasound Med Biol 1978; 3:388-392.
21. Fried AM, Cosgrove DO, Nassiri DK, McCready VR. The diaphragmatic echo complex: an in vitro-study. Invest Radiol 1985; 20:62-67.
22. Muller N, Cooperberg PL, Rowley VA, et al. Ultrasonic refraction by the rectus abdominis muscles: the double image artefact. J Ultrasound Med 1984; 3:515-520.
23. Sauerbrei EE. The split image artefact in pelvic ultrasonography: anatomy and physics. J Ultrasound Med 1985; 4:29-34.
24. Jaffe CC, Taylor KJW. The clinical impact of ultrasonic beam focusing patterns. Radiology 1979; 131:469-472.
25. Fiske CE, Filly RA. Pseudo-sludge. Radiology 1982; 144:631-632.
26. Reading CC, Charboneau JW, James EM, et al. Sonographically guided percutaneous biopsy of small (3cm or less) masses. Am J Roentgenol 1988; 151:189-192.
27. Shiina S, Tagawa K, Niwa Y, et al. Percutaneous ethanol injection therapy for hepatocellular carcinoma: results in 146 patients. Am J Roentgenol 1993; 160:1023-1028.
28. Amin Z, Donale J, Masters A, et al. Hepatic metastases: interstitial laser photocoagulation with real-time US monitoring and dynamic CT evaluation of treatment. Radiology 1998; 187:339-347.
29. Dong B, Liang P, Yu X, et al. Sonographically-guided microwave coagulation treatment of liver cancer: an experimental and clinical study. Am J Roentgenol 1998; 171: 449-454.
30. Livraghi T, Goldberg SN, Lazzaroni S, et al. Small hepatocellular carcinoma: treatment with radio-frequency ablation versus ethanol injection. Radiology 1999; 210:655-661.